Ternary Non-Fullerene Polymer Solar Cells with 13.51% Efficiency and a Record-High Fill Factor of 78.13%

Journal:	*Energy & Environmental Science*
Manuscript ID	EE-ART-05-2018-001564.R1
Article Type:	Paper
Date Submitted by the Author:	05-Jul-2018

Complete List of Authors:	Nian, Li; South China Normal University, South China Academy of Advanced Optoelectronics Kan, Yuanyuan; University of Washington Wang, Haitao; South China University of Technology Gao, Ke; University of washington, Xu, Bo; KTH-Royal Institute of Technology, Department of Chemistry Rong, Qikun; South China Normal University, Wang, Rong; South China University of Technology Wang, Jing; Shanghai Jiao Tong University Liu, Feng; Shanghai Jiao Tong University Chen, Junwu; South China University of Technology, Institute of Polymer Optoelectronic Materials and Devices Zhou, Guofu; South China Normal University Russell, Thomas; University of Massachusetts, Polymer Science and Engineering Department Jen, Alex K-Y.; University of Washington, Materials Science and Engineering; University of Washington, Chemistry

Journal Name

ARTICLE

Ternary Non-Fullerene Polymer Solar Cells with 13.51% Efficiency and a Record-High Fill Factor of 78.13%

Received 00th January 20xx,
Accepted 00th January 20xx

DOI: 10.1039/x0xx00000x

www.rsc.org/

Li Nian,*[‡ag] Yuanyuan Kan,[‡b] Haitao Wang,[c] Ke Gao,[b] Bo Xu,[b] Qikun Rong,[ag] Rong Wang,[c] Jing Wang,[d] Feng Liu,*[d] Junwu Chen,*[c] Guofu Zhou,*[ag] Thomas P. Russell[e] and Alex K.-Y. Jen*[bf]

Non-fullerene polymer solar cells (NF PSCs) have attracted much attention in recent years due to their rapidly increasing power conversion efficiency (PCE). In this work, two highly efficient ternary NF PSCs with FFs over 78% and PCEs up to 13.52% and 12.70% are demonstrated by adding a strongly aggregating polymer P1 into the classic PBDB-T:IT-M and PBDB-T:ITIC non-fullerene blends. The addition of P1 significantly enhances the crystallization of the blend film, while maintains the desired morphology. The ternary devices show highly improved charge extraction and suppressed charge recombination in comparison to the binary mixture. The PCE of the PBDB-T:ITIC based NF PSC was found to increase from 10.82% to 12.70% and FF from 71.85% to 78.07% after adding P1. For PBDB-T:IT-M based NF PSC, the PCE increases from 11.71% to 13.52% and FF from 72.07% to 77.83%. The high FFs and PCEs are the best results reported for ternary NF PSCs to date.

Introduction

Polymer solar cells (PSCs) are one of the promising and cost-effective alternatives for future renewable energy due to their unique advantages of low-cost, light-weight and flexible form factors.[1-10] Recently, ternary mixtures, that use either two electron donor polymers or two electron acceptors, have been widely used to elevate the power conversion efficiency (PCE) of PSCs.[11-15] In ternary PSCs, the light harvesting ability of the active layer can be enhanced markedly by the additional absorber with complementary absorption spectrum, resulting in much improved short-circuit current density (J_{sc}).[16-18] High J_{sc} over 25 mA cm^{-2} have been demonstrated in ternary blend.[18] Meanwhile, the open-circuit voltage (V_{oc}) in ternary PSCs can be continuously tuned by varying the donor or acceptor compositions, rather than be pinned to the lower V_{oc} of the binary blends.[19-21] By combining experiments and modelling, Kemerink and co-workers demonstrated that the enhanced absorption by introducing an additional component offered modest improvements over binary devices while the increased fill factor (FF) arising from the improved charge transport and recombination may offer more significant contributions to the enhanced device performance.[22] However, the FF for ternary PSCs is the least controllable among the three parameters since the FF for PSCs can be influenced by many factors, and the third component makes the dynamic process in ternary blend more complex. For many ternary PSCs reported, although the PCEs can be improved due to the increased J_{sc}, the FFs for the devices often stay unchanged or even reduced when the third component is introduced, due to the formation of energetic traps and disruption of molecular packing.[23] To date, the FFs for state-of-the-art ternary PSCs with PCEs over 10% are mostly below 75% (**Table S1**), leaving ample room for further improvement.

Generally, the FF of a PSC is determined by the competition between charge transport/extraction and recombination. An efficient way to improve these processes simultaneously is to increase the crystallization (but with reasonable domains size to ensure exciton dissociation) of the active layer.[24] Highly crystalline materials/domain show higher charge carrier mobility and better domain purity, which will facilitate the charge extraction and reduce charge carrier recombination in the active layer. For instance, by using a highly crystalline

[a] *Guangdong Provincial Key Laboratory of Optical Information Materials and Technology & Institute of Electronic Paper Displays, South China Academy of Advanced Optoelectronics, South China Normal University, Guangzhou 510006, P. R. China. Email: nianli@m.scnu.edu.cn; guofu.zhou@m.scnu.edu.cn*
[b] *Department of Materials Science and Engineering, University of Washington, Seattle, WA 98195, USA. Email: ajen@uw.edu*
[c] *Institute of Polymer Optoelectronic Materials and Devices, State Key Laboratory of Luminescent Materials and Devices, South China University of Technology, Guangzhou 510640, P. R. China. Email: psjwchen@scut.edu.cn*
[d] *Department of Physics and Astronomy, and Collaborative Innovation Center of IFSA (CICIFSA), Shanghai Jiaotong University, Shanghai 200240, P. R. China. E-mail: fengliu82@sjtu.edu.cn*
[e] *Materials Sciences Division, Lawrence Berkeley National Lab, Berkeley, CA, 94720, USA.*
[f] *Department of Chemistry, City University of Hong Kong, Kowloon, Hong Kong, SAR, P. R. China*
[g] *National Center for International Research on Green Optoelectronics, South China Normal University, Guangzhou 510006, P. R. China*
† Electronic Supplementary Information (ESI) available: [Experimental details, GIWAXS, J-V curves, EQE spectra, AFM images, SCLC measurements]. See DOI: 10.1039/x0xx00000x
‡ These authors contributed equally to this work.

polymer (PffBT4T-2OD and PTPD3T) or a highly crystalline non-fullerene acceptor (IDTN) with corresponding fullerene acceptor or polymer donor, high FF of 77%, 79.6% and 78% were achieved in binary PSCs, respectively.[24-26] In addition, the

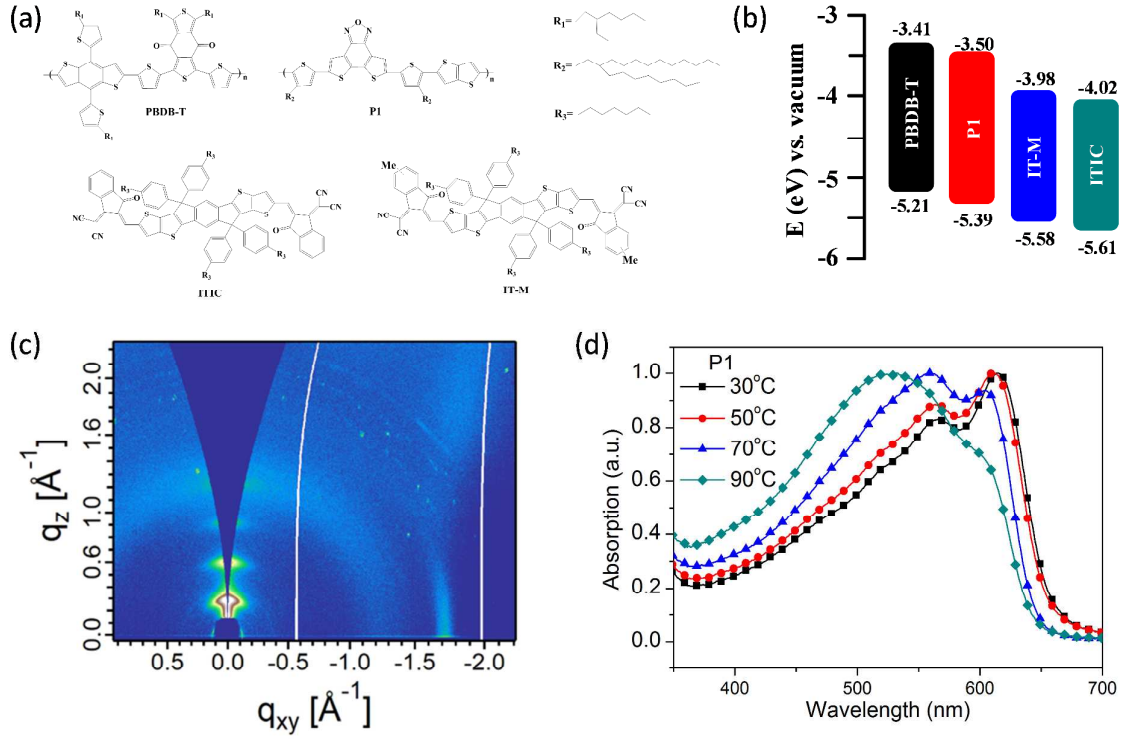

Fig. 1 (a) Chemical structures and (b) Energy level diagrams of PBDB-T, P1, ITIC and IT-M. (c) Grazing incidence wide-angle X-ray scattering pattern of pure P1 film. (d) Temperature-dependent absorption spectra of P1 in chlorobenzene solution with a concentration of 1×10^{-5} M.

commonly used device optimization methods to improve the FF,

such as thermal annealing, solvent-vapor annealing and solvent additive, are also aiming at optimizing the crystallization or ordered molecular packing in the active layer.[27-29] Hence, the development/selection of a suitable third component to improve the process of crystallization in the active layer while maintain a proper sized phase separation is of great importance for further FF and PCE breakthroughs in ternary PSCs.

In this work, we demonstrate two highly efficient ternary non-fullerene (NF) PSCs with FFs over 78% and PCEs up to 13.52% and 12.70%, respectively. P1 (also known as PDTfBO-TT), a strongly aggregating polymer with a hole mobility of 0.54 cm^2 V^{-1} s^{-1}, is used as the additional donor into PBDB-T:ITIC and PBDB-T:IT-M blends.[30] The addition of P1 significantly enhances the crystallization of the blend film while maintains proper morphology. The ternary devices show highly improved charge extraction and suppressed charge recombination in comparison to the binary mixture. As a result, the PCE of the PBDB-T:ITIC based NF PSC increases from 10.82% to 12.70% and FF from 71.85% to 78.07% after adding P1. For PBDB-T:IT-M based NF PSC, the PCE increases from 11.71% to 13.52% and FF from 72.07% to 77.83%. The high FFs and PCEs are the best results reported for ternary NF PSCs to date.

Results and Discussion

The chemical structures of PBDB-T, P1, ITIC and IT-M are shown in **Figure 1a**. **Figure 1b** shows their energy levels reported in previously studies.[30-32] We have employed photoluminescence (PL) spectroscopy to study the possible charge/energy transfer between PBDB-T and P1 by measuring the PL signal of PBDB-T, P1 and PBDB-T:P1 blended films as shown in **Figure S1**. The increased PL signal of PBDB-T, concomitant with a quenching of P1 PL signal in blends, provides evidence for the energy transfer process from P1 to PBDB-T. The energy transfer contributes to the extraction of inner P1 excitons (if the small amount of P1 blended in PBDB-T), followed by efficient charge separation at PBDB-T: ITIC or PBDB-T :IT-M interface.[33] **Figure 1c** shows the grazing incidence wide-angle x-ray scattering (GIWAXS) of pure P1. Three orders of diffraction characteristic of the alkyl-to-alkyl (center-to-center distance) stacking are seen, indicating that P1 is a strongly crystallizing polymer. The strong aggregation property of P1 is also confirmed by the temperature-dependent absorption spectra (**Figure 1d**), in which the P1 solution (10^{-5} M in chlorobenzene) still showed a shoulder perk at 90 °C.

BHJ thin film structure order was studied by GIWAXS, with diffraction patterns and line-cut profiles shown in **Figure 2**. GIWAXS of the pure film of PBDB-T, ITIC and IT-M are shown in **Figure S2**. PBDB-T is a semi-crystalline polymer with a well-defined lamellae and π-π stacking. However, when blended with ITIC, even though processed with DIO additive, a poor structure order is seen. Weak and broad polymer (100) diffraction is observed and enhanced in out-of-plane direction at 0.29 $Å^{-1}$. The π-π stacking is observed at 1.73 $Å^{-1}$. The

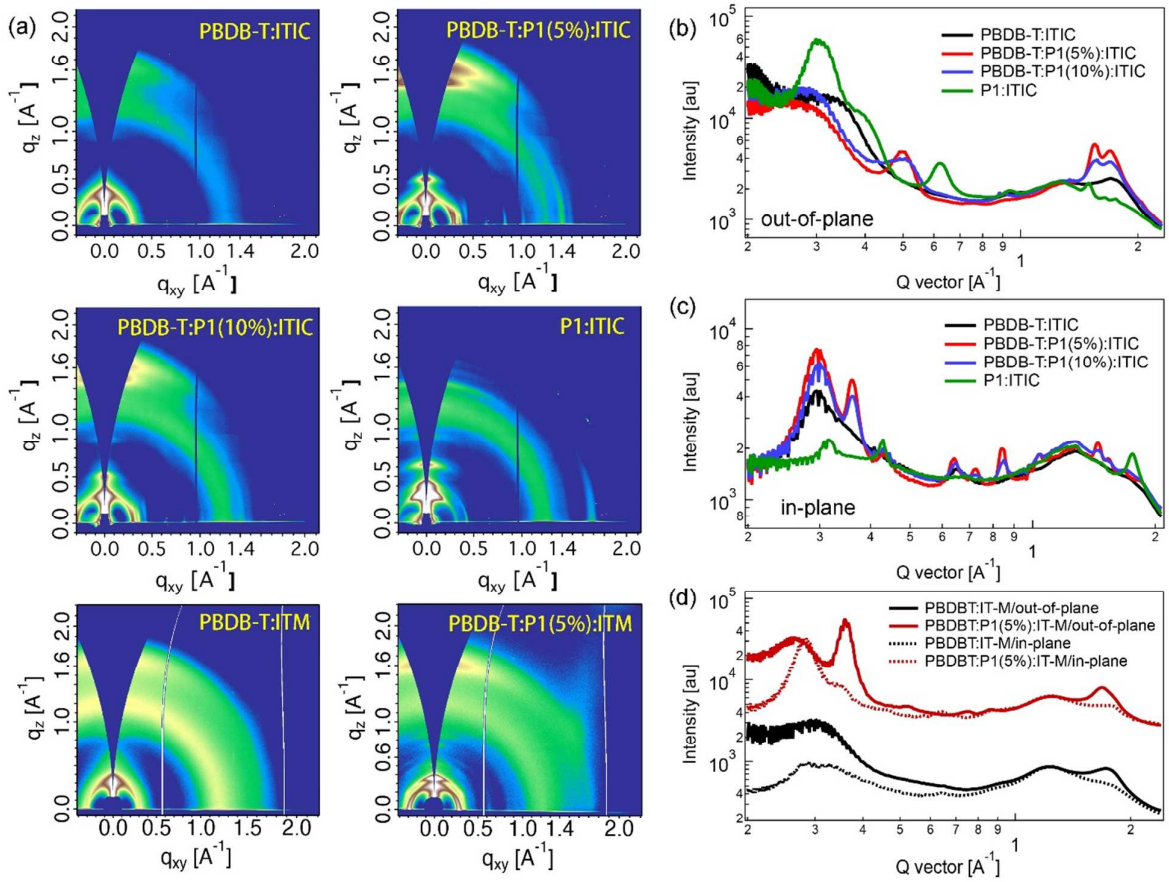

Fig. 2 a) Grazing incidence wide-angle X-ray scattering pattern, b) out-of-plane line-cut profiles of ITIC based BHJ blends; c) in-plane line-cut profiles of ITIC based BHJ blends; d) line-cut profiles of IT-M based BHJ blends (solid line: out-of-plane profile; dotted line: in-plane profile)

crystallization of ITIC is fully suppressed by the presence of PBDB-T, indicating a good mixing of these two components. Binary blends of P1:ITIC thin film shows quite strong crystallization of the conjugated polymers, showing 3 orders of alkyl-to-alkyl interaction peaks (0.31 $Å^{-1}$). Its π-π stacking peak is located in the in-plane direction at 1.76 $Å^{-1}$, coming from P1. Thus, P1 could also retard the crystallization of ITIC, forming mixed regions to facilitate electron transport.

However, when ternary blend was used, BHJ thin films showed quite prominent ordering of ITIC. With 5% addition of P1 (the mass ratio of P1 in overall donors, similarly hereinafter), a new diffraction at 0.50 $Å^{-1}$ in the out-of-plane direction and 0.37 $Å^{-1}$ diffraction in the in-plane direction are seen, corresponding to different packing motif of ITIC. Polymer (100) diffraction is remained at 0.29 $Å^{-1}$, dominated by PBDB-T structure features. The polymer (100) diffraction became sharper and more intense, and thus PBDB-T crystallization and size got enhanced. Quite strong π-π stacking diffractions of ITIC are seen in the out-of-plane direction, located at 1.55 $Å^{-1}$ and 1.72 $Å^{-1}$, corresponding to different packing of ITIC. Such a feature can enhance the transport of both electrons and holes, leading to improved FF in device. Adding more P1 (10%) in the ternary blend yields similar diffraction features. However, as seen from the π-π stacking region, the peak intensity is reduced when more P1 (10%) is added, but it is still greater than that for the binary blend. Although P1 itself cannot induce a face-on ordering of ITIC, as seen from P1:ITIC blends GIWAXS data, its mixture with PBDB-T changed the fundamental physical properties, which allows ITIC more readily to order. Therefore, higher transport can be achieved to improve device performance. When using IT-M as the acceptor in binary and ternary blends, adding 5% of P1 also significantly improves the crystallization, as seen from the sharp increase and narrowing of the PBDB-T (100) peak that has a crystalline correlation length (CCL) of 17.5 nm. The π-π stacking also improves, where the peak position slightly shifts to lower q for the PBDB-T:P1:IT-M blends.

The morphologies of the PBDB-T: P1: ITIC films were studied using atomic force spectroscopy (AFM), transmission electron microscopy (TEM) and resonant soft x-ray scattering (RSoXS) as shown in **Figure 3**. As can be seen from the AFM and TEM images, all films show a uniform morphology with some fibrillar textures. From the AFM images, the root-mean-square roughness (RMS) increases from 1.97 nm for PBDB-T: ITIC blend

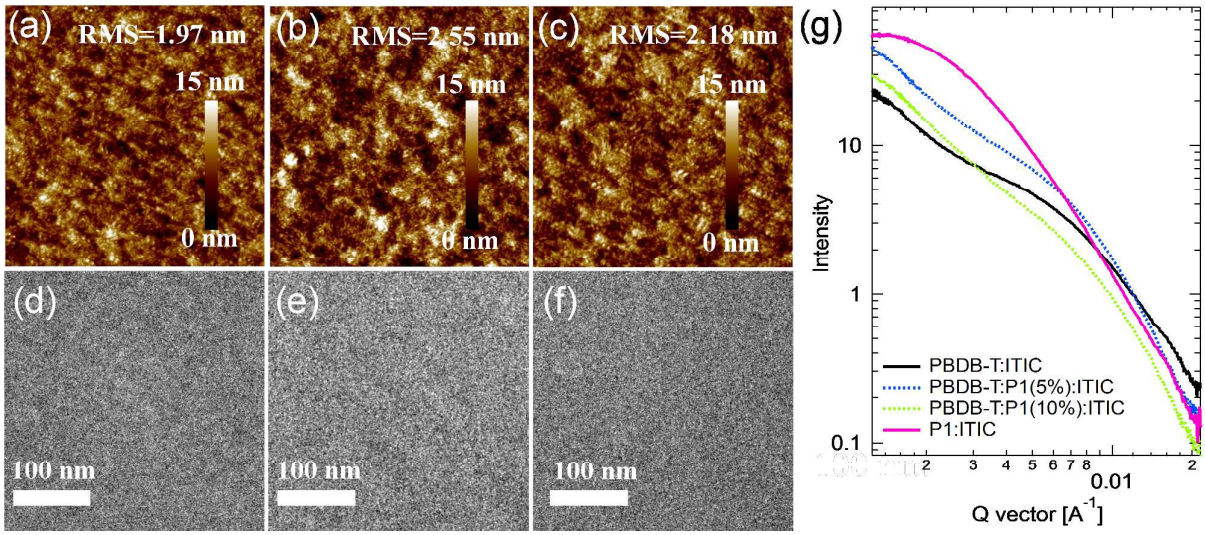

Fig. 3 AFM height images (a-c) and TEM images (d-f) for PBDB-T: P1: ITIC with 0%, 5%, and 10% P1 content from left to right. (g) resonant soft X-ray scattering of BHJ blends under different conditions. The scan size is 5μm × 5μm for all AFM images.

to 2.55 nm for the 5% ternary blend and 2.18 nm for the 10% ternary blend, which is consistent with the increased ternary blends showed similar morphologies with the binary blend. The AFM phase images are shown in **Figure S3**. The phase separation of BHJ thin film were investigated by RSoXS. All BHJ thin films showed quite broad scattering profiles, indicating a multi-length scaled morphology. PBDB-T:ITIC blends showed a small length scale of phase separation at ~0.006 A^{-1}, giving a distance of 105 nm by using double tangent lines to estimate peak positions. P1:ITIC blends showed a phase separation ~300 nm, which is much larger than the ideal length scale. Ternary blends showed scattering hump similar to that of PBDB-T:ITIC blends, and thus the small length scaled phase separation was locked by PBDB-T:ITIC blends. The 5% ternary blends showed the best scattering intensity, and thus the most pronounced phase separation. Debye Bucherer model was used to fit the RSoXS data, which yield correlation length of 15.2, 14.4, 12.5, and 38.1 nm for PBDB-T:ITIC, PBDB-T:P1(5%):ITIC, PBDB-T:P1(10%):ITIC, and P1:ITIC respectively. Thus, adding P1 into BHJ blends could reduce the size of phase separation. Thus, the improved crystallinity and smaller length scale of phase separation reflects a more optimal morphology for this ternary blend, and an improved device efficiency is expected.

Since the addition of P1 into the binary blend could enhance crystallization while maintain a proper morphology, it is reasonable to use the ternary blend to fabricate ternary PSCs. The photovoltaic performance of the ternary PSCs were investigated based on the following device structure: ITO/ ZnO/ PFN/ PBDB-T: P1: IT-X (ITIC or IT-M)/ MoO_3/ Al. The overall donors to acceptors ratio were kept at 1:1 in this study. Poly[(9,9-bis(3′-(N,N-dimethylamino)propyl)-2,7-fluorene)-alt-2,7-(9,9-dioctylfluore ne)] (PFN) was used to improve the device performance and its structure is shown in **Figure S4**. The photovoltaic parameters of the devices are shown in **Table 1**. **Figure 4a** illustrates the representative current density versus voltage (J-V) characteristics of devices with different PBDB-T: P1 weight ratios (0%, 5% and 10% P1) under simulated AM 1.5 G illumination at 100 mW cm^{-2}.

The PBDB-T: ITIC binary control devices exhibit an average PCE (PCE_{ave}) of 10.66±0.10% with a V_{oc} of 0.90±0.00V, a J_{sc} of 16.64±0.16 mA cm^{-2} and a FF of 71.24±0.54%. Adding 5% of P1 (the amount of P1 added to the donor, hereinafter) into the PBDB-T: ITIC blend dramatically increases the J_{sc} to 17.98±0.15 mA cm^{-2} and FF to 77.33±0.66%, resulting in a promising PCE_{ave} of 12.51±0.12%. Further addition of P1 (10%) led to a decreased in the J_{sc} (17.48±0.17 mA cm^{-2}) and FF (75.78±0.72%), but the PCE remained higher (11.92±0.13%) than that of the PBDB-T: ITIC blend. These results show that using a small amount of strongly aggregating polymer to enhance the crystallization of the active layer can dramatically improve the ternary device performance. The P1: ITIC binary device was also fabricated and it showed a low PCE of 3.85±0.37%, due to the much lower J_{sc} and FF (**Figure S5**) caused by too large phase separation and surface roughness (**Figure S6**). For PBDB-T: IT-M blend, 5% P1 addition shows a similar behaviour to that of PBDB-T:ITIC blend, enhancing the PCE from 11.57±0.09% to 13.31±0.14% and FF from 71.46±0.56% to 76.86±0.79%.

External quantum efficiency (EQE) measurements were conducted to confirm the J_{sc} of the PSCs. As shown in **Figure 4b**, the ternary blend based devices show remarkable enhancement in comparison to the corresponding control devices, contributing to the increased J_{sc} value. The much improved charge carrier collection and reduced recombination contribute to the enhanced EQE values which will be discussed below. The integrated J_{sc} values from EQE measurements were shown in Table 1, agreeing well with J-V measurements (the deviations are within 3%).To further confirm the effect of 5%

P1 addition, the statistical FF distribution histograms of the 5% P1

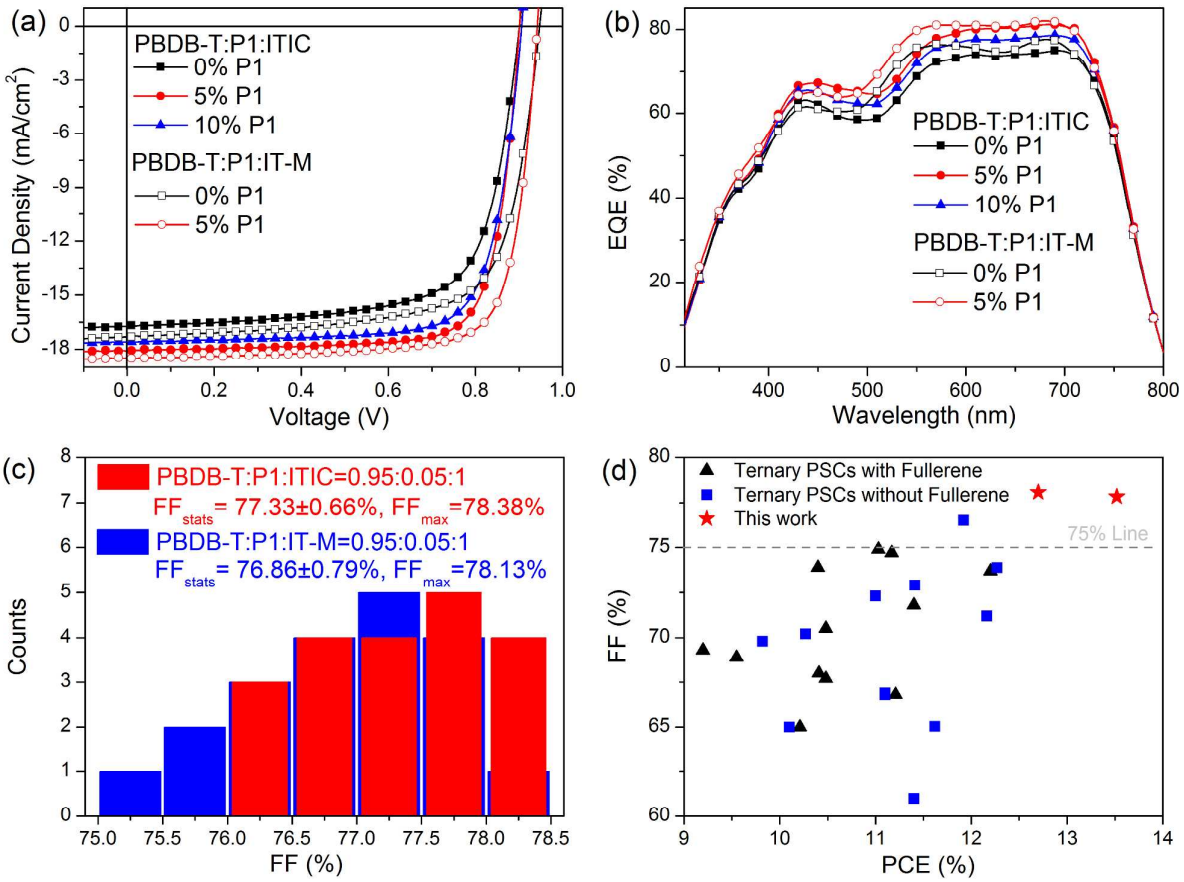

Fig. 4 (a) Current density versus voltage characteristics and (b) EQE curves of the devices with 0%, 5% and 10% P1 content in donor. Device structure: ITO/ ZnO/ PFN/ PBDB-T: P1: IT-X (ITIC or IT-M)/ MoO_3/ Al. (c) Statistical FF distribution histogram of the optimized ternary PSCs based on 20 cells. (d) The FF values of ternary PSCs with PCEs over 9%.

ternary PSCs based on PBDB-T: ITIC and PBDB-T: IT-M are shown in **Figure 4c**. The average FF are calculated from 20 identical devices prepared from different batches. The J-V curves and photovoltaic parameters of these ternary devices are summarized in **Figure S7** and **Table S2-S3**. Both of the ternary systems show FF_{max} over78%, which are the highest FF value reported for ternary NF PSCs to date.

To understand the high FF values achieved in the PBDB-T: P1: ITIC ternary blend, the charge transport and extraction properties were investigated initially. Charge carrier mobility was measured by using the space-charge-limited-current (SCLC) method (**Figure S8**). The hole-only devices and electron-only devices were fabricated by using the device architectures of ITO/ PEDOT:PSS/ active layer/ MoO_3/ Au and Al/ active layer/ Ca/ Al, respectively. The mobility is extracted from the slopes of $J^{1/2}$-V curves by modelling the dark current in the SCLC region. The hole mobilities of the PBDB-T: P1: ITIC= (1:0:1), (0.95:0.05:1) and (0.9:0.1:1) devices are 1.8×10^{-4}, 4.7×10^{-4} and 3.7×10^{-4} cm^2 V^{-1} s^{-1}, respectively, while the electron mobilities of them are 2.3×10^{-4}, 6.4×10^{-4} and 4.9×10^{-4} cm^2 V^{-1} s^{-1}, respectively. The increased crystallinity arising from the P1 addition contributed to the much increased hole and electron mobilities, leading to a better FF for device.

The detailed information about the charge extraction process in devices was probed by using transient photocurrent (TPC) measurement (**Figure 5a**). The charge extraction time decreased from 0.29 μs for PBDB-T: ITIC blend to 0.13 μs for 5% ternary blend and 0.18 μs for 10% ternary blend, respectively. The reduced charge extraction time in the ternary device indicates more efficient charge extraction from the active layer, which is beneficial to the improvement in J_{sc} and FF. The charge recombination dynamics in devices were probed using transient photovoltage (TPV) measurements. **Figure S9** shows the typical results of TPV measurement for PBDB-T: P1: ITIC=1:0:1, 0.95:0.05:1 and 0.9:0.1:1 devices. The extracted charge carrier lifetime increased from 2.04 μs for PBDB-T:ITIC device to 4.18 μs for PBDB-T: P1: ITIC (5% P1) device and 3.36 μs for PBDB-T: P1: ITIC (10% P1) device. The observed longer carrier lifetime suggested a reduced bimolecular recombination loss in the P1 adding devices, which is beneficial to the FF and J_{sc} values for the ternary device.

To gain more insight into the exciton dissociation and charge extraction, we measured the photocurrent density (J_{ph}) as a function of the effective voltage (V_{eff}) as shown in **Figure 5b**.[34] $J_{ph} = J_L - J_D$, where J_L and J_D are the current densities under illumination and in dark, respectively. $V_{eff} = V_0 - V_A$, where V_0 is

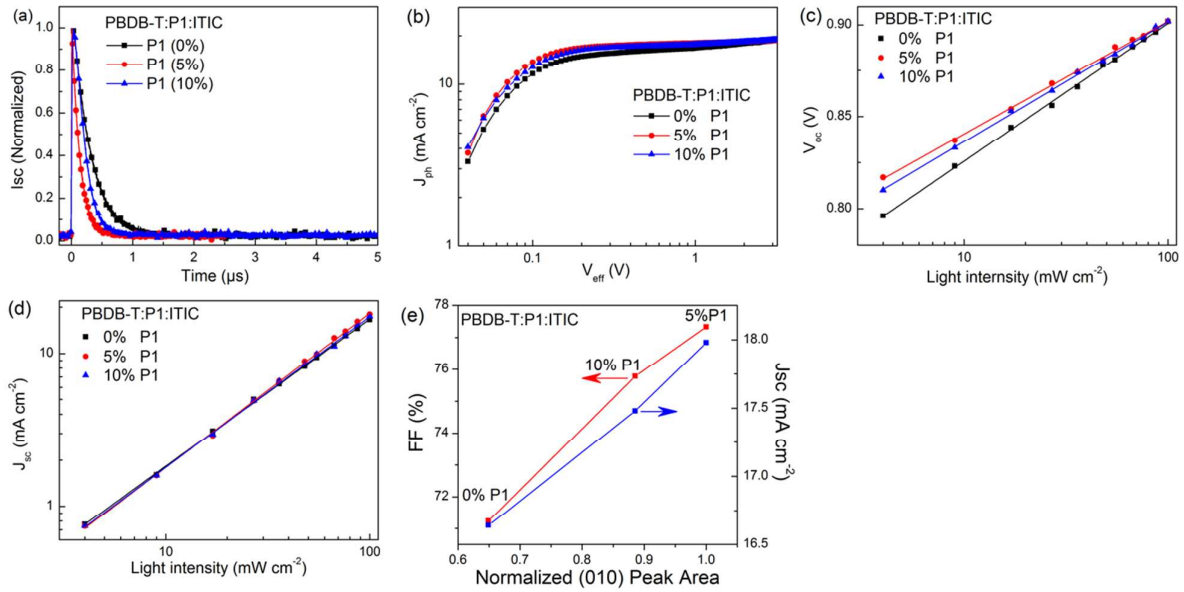

Fig. 5 (a) Transient photocurrent measurements, (b) Photocurrent density (J_{ph}) versus effective voltage (V_{eff}) curves, (c) Dependence of V_{oc} on light intensity and (d) Dependence of J_{sc} on light intensity for the devices with 0%, 5% and 10% P1 content. (e) FF and J_{sc} versus normalized (010) peak area for PBDB-T:P1:ITIC devices with 0%, 5% and 10 P1 content.

Table 1. The photovoltaic parameters for PBDB-T:P1:IT-X (ITIC or IT-M) devices under simulated AM 1.5 G illumination at 100 mW cm^{-2}.

P1 (%)	Acceptor	V_{oc} [V][a)]	J_{sc} [mA cm^{-2}][a)]	J_{calc} [mA cm^{-2}][b)]	FF [%][a)]	PCE [%][a) c)]
0	ITIC	0.90±0.00	16.64±0.16	16.50	71.24±0.54	10.66±0.10 (10.82)
5	ITIC	0.90±0.00	17.98±0.15	17.79	77.33±0.66	12.51±0.12 (12.70)
10	ITIC	0.90±0.01	17.48±0.17	17.28	75.78±0.72	11.92±0.13 (12.13)
100	ITIC	0.93±0.01	8.15±0.32	8.38	54.44±1.32	3.85±0.37 (4.42)
0	IT-M	0.94±0.00	17.17±0.14	17.13	71.46±0.56	11.57±0.09 (11.71)
5	IT-M	0.94±0.00	18.42±0.09	18.16	76.86±0.79	13.31±0.14 (13.52)

[a)] All average values with standard deviations were calculated from 20 devices; [b)] J_{sc} integrated from the EQE spectrum; [c)] Best PCE in the bracket.

the zero J_{ph} voltage and V_A is the applied bias voltage. At high V_{eff} (3.2V in this study), it is assumed that all of the generated excitons are dissociated and collected at the electrodes, resulted in a saturation current (J_{sat}). The charge collection probability P(E, T) is determined by normalizing J_{ph} with J_{sat}. The P(E,T) values under short circuit condition for PBDB-T: P1: ITIC=(1:0:1), (0.95:0.05:1) and (0.9:0.1:1) devices are 88.85%, 96.27% and 93.46%, respectively. More interestingly, the P(E,T) at the maximum power point (M_{pp}) dramatically increases from 75.46% to 89.03% (5% P1) and to 84.80% (10% P1). The higher P(E,T) value for the ternary blend device again suggests that the P1 addition is efficient in promoting charge extraction, leading to an increased J_{sc} and a record-high FF>78% for the ternary PSCs. The enhanced crystallization and charge carrier mobilities in the ternary blend device contribute to the increased charge extraction.

We next analysed the charge recombination behaviour of the binary and ternary devices to understand the high FF by measuring J_{sc} and V_{oc} as a function of the light intensity (P_{light}). At V_{oc} conditions, all of the charge carriers recombine inside the active layer and the recombination mechanism can be studied by analysing the slope of V_{oc} versus the natural logarithm of P_{light}.[35] For bimolecular recombination system, the slope is close to k_BT/q (k_B is Boltzmann's constant, T is absolute temperature and q is the elementary charge). For trap-assisted recombination system, the V_{oc} shows enhanced dependence on the P_{light} ($2k_BT/q$). As shown in **Figure 5c**, the slope deceases from $1.26k_BT/q$ for PBDB-T: ITIC control device to $1.03k_BT/q$ for the 5% ternary device and to 1.10 k_BT/q for the 10% ternary device, indicating that the P1 addition suppresses the trap-assisted recombination. The decreased trap-assisted recombination may arise from a decrease in the

trap density due to the enhanced crystallinity of the active layer.

Since the bimolecular recombination is the dominant charge loss mechanism (the slopes are close to k_BT/q rather than 2 k_BT/q as mentioned above), we analysed the relationship between J_{sc} and P_{light} to evaluate the degree of the bimolecular recombination in the devices.[36] In PSCs, J_{sc} has a power-law dependence on light intensity $J_{sc} \propto (P_{light})^S$. For a device with weak bimolecular recombination, the S value is closed to 1. **Figure 5d** showed the $J_{sc} \sim P_{light}$ relationship for PBDB-T: P1: ITIC= (1:0:1), (0.95:0.05:1) and (0.9:0.1:1) devices. The extracted S values are 0.960, 0.999 and 0.984, respectively, indicating that bimolecular recombination is highly restrained in the devices with 5% P1 content. Therefore, both trap-assisted recombination and bimolecular recombination are highly suppressed in the 5% ternary devices, which are dominant factors contributing to the state-of-the-art FF values.

Figure 5e shows the relationship between the FF and J_{sc} as a function of the normalized area of the (010) reflection for PBDB-T:P1:ITIC devices. The normalized (010) peak area for 5% P1 and 10% P1 ternary devices are 54% and 36% greater than that for PBDB-T:ITIC binary blend. The FF and J_{sc} values correlate well with the (010) peak area, which is consist with the findings of Hou and co-workers.[37] The result shown here show that the strategy of using a strongly aggregating polymer to enhance the crystallization of the active layer can remarkably improve the device performance.

To prove the general applicability of our method, we have used two other strongly aggregating polymers, P2 and P3 (also known as PDTfBO-DT and PDTfBO-T) as the additional donor into PBDB-T:ITIC blend. The chemical structures of P1, P2, and P3 are shown in **Figure S10**. As shown in our previously study,[30] P1 and P2 showed similar aggregation ability while P3 shows much stronger aggregation ability compared to P1 and P2, deduced from their de-aggregation behaviors during heating process. **Figure S10** illustrates the representative J-V characteristics of devices based on PBDB-T: PX (P1, P2 or P3): ITIC under simulated AM 1.5 G illumination at 100 mW cm^{-2}. The mass ratio of PX in each donor is kept at 5%. The best photovoltaic parameters of the devices are shown in **Table S4**. Although the device with P1 addition gives the best photovoltaic performance, the P2 addition also leads to greatly improved performance. However, the addition of P3 decreases the J_{sc} and FF in device, which may be due to the too strong aggregation nature of P3. These results showed that using strongly aggregating polymers as the third component could be an effective method to improve the device performance and the aggregation ability of the blend should be well-tuned to optimize the improvement.

Conclusions

In conclusion, high efficiency ternary non-fullerene solar cells were fabricated by adding a small amount of P1 into PBDB-T: ITIC and PBDB-T: IT-M mixtures. The small portion of added P1 does not change the length scale of the phase separation of the PBDB-T: ITIC, but the ordering is much improved and the donor and acceptors showed enhancement in the hole and electron mobilities. More interestingly, such a modification leads to an impressive improvement in the device FF to over 78%. Enhanced charge transport also contributes to elevated charge collection, and the short circuit current density is markedly improved. Impressive 12.70% PCE and 78.07% FF could be obtained for a traditional non-fullerene PBDB-T:ITIC mixture and 13.52% PCE and 77.83% FF could be achieved in PBDB-T:IT-M blend, which are the highest reported to date, showing the importance of fine-tuning the crystallization of ternary blend film.

Conflicts of interest

There are no conflicts to declare.

Author Contributions

L.N. conceived the idea. Device fabrication and characterization were carried out by L. N. The design of experiments, discussion of results and manuscript writing were done by L. N., F. L., J. C., G. Z., T. P. R. and A. K.-Y. J. The donor of P1 was synthesized by H. W.. Y. K., K. G., B. X., Q. R., R. W. and J. W. were contributed to the device measurement and analysis of data. All the authors discussed the results and contributed to the writing of the manuscript.

Acknowledgements

This work was financially supported by National Key R&D Program of China (2016YFB0401501), National Natural Science Foundation of China (51561135014, U1501244). Program for Changjiang Scholars and Innovative Research Teams in Universities (No. IRT_17R40), Guangdong Innovative Research Team Program (No. 2013C102), Guangdong Provincial Key Laboratory of Optical Information Materials and Technology (Grant No. 2017B030301007), MOE International Laboratory for Optical Information Technologies and the 111 project. A. K.-Y. J. acknowledges financial support from the Asian Office of Aerospace R&D (FA2386-15-1-4106) and the Office of Naval Research (N00014-17-1-2201, N00014-14-1-0246, N00014-17-1-2260). J. C. acknowledges financial support from National Natural Science Foundation of China (U1401244) and the National Basic Research Program of China (973 program 2014CB643505). F.L. was supported by the Young 1000 Talents Global Recruitment Program of China. T.P.R were supported by the U.S. Office of Naval Research under contract N00014-17-1-2244. Portions of this research were carried out at beamline 7.3.3 and 11.0.1.2 at the Advanced Light Source, and Molecular Foundry, Lawrence Berkeley National Laboratory, which was supported by the DOE, Office of Science, and Office of Basic Energy Sciences.

Notes and references

1 L. Dou, J. You, J. Yang, C.- C. Chen, Y. He, S. Murase, T. Moriarty, K. Emery, G. Li and Y. Yang, *Nat. Photonics*, 2012, **6**, 180.
2 Y. Cui, H. Yao, B. Gao, Y. Qin, S. Zhang, B. Yang, C. He, B. Xu and J. Hou, *J. Am. Chem. Soc.*, 2017, **139**, 7302.
3 J. Zhao, Y. Li, G. Yang, K. Jiang, H. Lin, H. Ade, W. Ma and H. Yan, *Nat. Energy*, 2016, **1**, 15027.
4 L. Nian, W. Zhang, N. Zhu, L. Liu, Z. Xie, H. Wu, F. Würthner and Y. Ma, *J. Am. Chem. Soc.*, 2015, **137**, 6995.
5 L. H. Rossander, H. F. Dam, J. E. Carlé, M. Helgesen, L. Rajkovic, M. Corazza, F. C. Krebs and J. W. Andreasen, *Energy Environ. Sci.*, 2017, **10**, 2411.
6 J. Wan, X. Xu, G. Zhang, Y. Li, K. Feng and Q. Peng, *Energy Environ. Sci.*, 2017, **10**, 1739.
7 L. Nian, Z. Chen, S. Herbst, Q. Li, C. Yu, X. Jiang, H. Dong, F. Li, L. Liu, F. Würthner, J. Chen, Z. Xie and Y. Ma, *Adv. Mater.*, 2016, **28**, 7521.
8 S.-J. Ko, Q. V. Hoang, C. E. Song, M. A. Uddin, E. Lim, S. Y. Park, B. H. Lee, S. Song, S.-J. Moon, S. Hwang, P.-Q. Morin, M. Leclerc, G. M. Su, M. L. Chabinyc, H. Y. Woo, W. S. Shin and J. Y. Kim, *Energy Environ. Sci.*, 2017, **10**, 1443.
9 L. Nian, K. Gao, Y. Jiang, Q. Rong, X. Hu, D. Yuan, F. Liu, X. Peng, T. P. Russell and G. Zhou, *Adv. Mater.*, 2017, **29**, 1700616.
10 A. Kuzmich, D. Padula, H. Ma and A. Troisi, *Energy Environ. Sci.*, 2017, **10**, 395.
11 N. Gasparini, X. Jiao, T. Heumueller, D. Baran, G. J. Matt, S. Fladischer, E. Spiecker, H. Ade, C. J. Brabec and T, Ameri, *Nature Energy*, 2016, **1**, 16118.
12 L. Nian, K. Gao, F. Liu, Y. Kan, X. Jiang, L. Liu, Z. Xie, X. Peng, T. P. Russell and Y. Ma, *Adv. Mater.*, 2016, **28**, 8184.
13 D. Baran, R. S. Ashraf, D. A. Hanifi, M. Abdelsamie, N. Gasparini, J. A. Röhr, S. Holliday, A. Wadsworth, S. Lockett, M. Neophytou, C. J. M. Emmott, J. Nelson, C. J. Brabec, A. Amassian, A. Salleo, T. Kirchartz, J. R. Durrant and I. McCulloch, *Nat. Mater.*, 2017, **16**, 363.
14 M. Zhang, W. Gao, F. Zhang, Y. Mi, W. Wang, Q. An, J. Wang, X. Ma, J. Miao, Z. Hu, X. Liu, J. Zhang and C. Yang, *Energy Environ. Sci.*, 2018, **11**, 841.
15 L. Lu, M. A. Kelly, W. You and L. Yu, *Nat. Photonics*, 2015, **9**, 491.
16 X. Xu, Z. Bi, W. Ma, Z. Wang, W. C. H. Choy, W. Wu, G. Zhang, Y. Li and Q. Peng, *Adv. Mater.*, 2017, **29**, 1704271.
17 W. Jiang, R. Yu, Z. Liu, R. Peng, D. Mi, L. Hong, Q. Wei, J. Hou, Y. Kuang and Z. Ge, *Adv. Mater.*, 2017, **29**, 1703005.
18 H. Yao, Y. Cui, R. Yu, B. Gao, H. Zhang and J. Hou, *Angew. Chem. Int. Ed.*, 2017, **56**, 3045.
19 P. P. Khlyabich, A. E. Rudenko, B. C. Thompson and Y.-L. Loo, *Adv. Funct. Mater.*, 2015, **25**, 5557.
20 R. A. Street, D. Davies, P. P. Khlyabich, B. Burkhart and B. C. Thompson, *J. Am. Chem. Soc.*, 2013, **135**, 986.
21 P. P. Khlyabich, B. Burkhart and B. C. Thompson, *J. Am. Chem. Soc.*, 2012, **134**, 9074.
22 N. Felekidis, E. Wang and M. Kemerink, *Energy Environ. Sci.*, 2016, **9**, 257.
23 W. Huang, P. Cheng, Y. Yang, G. Li and Y. Yang, *Adv. Mater.*, 2018, **30**, 1705706.
24 Y. Liu, J. Zhao, Z. Li, C. Mu, W. Ma, H. Hu, K. Jiang, H. Lin, H. Ade and H. Yan, *Nat Commun.*, 2014, **5**, 5293.
25 X. Guo, N. Zhou, S. J. Lou, J. Smith, D. B. Tice, J. W. Hennek, R. P. Ortiz, J. T. L. Navarrete, S. Li, J. Strzalka, L. X. Chen, R. P. H. Chang, A. Facchetti and T. J. Marks, *Nature Photonics*, 2013, **7**, 825.
26 S. Li, L. Ye, W. Zhao, X. Liu, J. Zhu, H. Ade and J. Hou, *Adv. Mater.*, 2017, **29**, 1704051.
27 W. Ma, C. Yang, X. Gong, K. Lee and A. J. Heeger, *Adv. Funct. Mater.* 2005, **15**, 1617.
28 K. Sun, Z. Xiao, E. Hanssen, M. F. G. Klein, H. H. Gam, M. Pfaff, D. Gerthsen, W. W. H. Wong and D. J. Jones, *J. Mater. Chem. A*, 2014, **2**, 9048.
29 X. Guo, C. Cui, M. Zhang, L. Huo, Y. Huang, J. Hou and Y. Li, *Energy Environ. Sci.*, 2012, **5**, 7943.
30 H. Wang, Y. Zhu, Z. Liu, L. Zhang, J. Chen and Y. Cao, *Org. Electronics*, 2016, **31**, 1.
31 W. Zhao, S. Li, S. Zhang, X. Liu and J. Hou, *Adv. Mater.*, 2016, **28**, 1604059.
32 S. Li, L. Ye, W. Zhao, S. Zhang, S. Mukherjee, H. Ade and J. Hou, *Adv. Mater.*, 2016, **28**, 9423.
33 V. Gupta, V. Bharti, M. Kumar, S. Chand and A. J. Heeger, *Adv. Mater.*, 2015, **27**, 4398.
34 L. Lu, Z. Luo, T. Xu and L. Yu, *Nano lett.*, 2012, **13**, 59.
35 L. J. A. Koster, V. D. Mihailetchi, R. Ramaker and P. W. M. Blom, *Appl. Phys. Lett.*, 2005, **86**, 123509.
36 I. Riedel, J. Parisi, V. Dyakonov, L. Lutsen, D. Vanderzande and J. C. Hummelen, *Adv. Funct. Mater.*, 2004, **14**, 38.
37 Z. Zheng, O. M. Awartani, B. Gautam, D. Liu, Y. Qin, W. Li, A. Bataller, K. Gundogdu, H. Ade and J. Hou, *Adv. Mater.*, 2016, **28**, 1604241.

Table of Contents

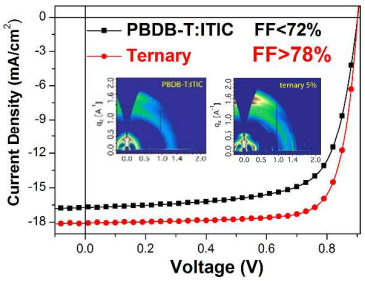

High PCEs and FFs are achieved in ternary non-fullerene PSCs by adding a strongly aggregating polymer into PBDB-T:IT-M and PBDB-T:ITIC.

Broader Context

Recently, ternary strategy has been widely used to improve the power conversion efficiency (PCE) of polymer solar cells (PSCs). In ternary PSCs, the short-circuit current density (J_{sc}) can be enhanced significantly by using a third component with complementary absorption spectrum. Meanwhile, the open-circuit voltage (V_{oc}) in ternary PSCs can be continuously tuned by varying compositions. However, the fill factor (FF) is still a bottleneck in ternary PSCs that needs to be improved especially those with non-fullerene (NF) due to the more complicated dynamic process. To date, the FFs for state-of-the-art ternary PSCs are mostly below 70%. In this work, a strongly aggregating polymer P1 is added into the classic PBDB-T:IT-M and PBDB-T:ITIC blends. The addition of P1 significantly enhances the crystallization of the blend film, and a clear structure-relationship is illustrated. The ternary devices show significantly improved charge extraction and suppressed charge recombination. As a result, the PCE of PBDB-T:ITIC based PSC increases from 10.82% to 12.70% and FF from 71.85% to 78.07% after adding P1. For PBDB-T:IT-M based PSC, the PCE increases from 11.71% to 13.51% and FF from 72.07% to 78.13%. The high FFs and PCEs are the best results reported to date for ternary NF PSCs.